Synchrotron radiation of relativistic runaway electrons

D. del-Castillo-Negrete, L. Carbajal

Oak Ridge National Laboratory, Oak Ridge, TN 37831-6169, USA

I. Introduction.

The study of synchrotron radiation (SR) of runaway electrons (RE) is important because SR provides a limiting mechanism for the maximum energy that RE can reach and also because it can be used as an experimental diagnostic to infer RE parameters including energy and pitch-angle distributions. Here we report recent results on SR taking into account full-orbit effects and the details of the SR camera geometry. The results were obtained using the recently developed SR synthetic diagnostic for the Kinetic Orbit Runaway electrons Code (KORC) [1,2] that computes the full-orbit relativistic dynamics in electric and magnetic fields including radiation damping and collisions. In Sec. II we consider SR of passing and trapped RE in axisymmetric fields, in Sec. III we study the role of magnetic stochasticity and islands on SR, and in Sec. IV we apply the KORC SR synthetic diagnostic to model RE in DIII-D quiescent plasmas.

II. Axisymmetric magnetic fields.

The SR of passing particles in an axisymmetric magnetic field is shown in Fig. 1 where the red dots in panel (a) denote the initial mono-pitch angle states and the corresponding initial total radiation power. The colored dots denote the final state of the RE. The collisionless pitch angle scattering [1,3] shown in panel (b) leads to the distribution of radiation power in panel (c). In general, for passing particles in axisymmetric fields, neglecting orbit effects might underestimate or overestimate the total radiation power depending on the direction of the radial shift of the drift orbits [1,3].

Figure 2 illustrates the role of particle trapping on SR for a mono-energetic, $\mathscr{E}_0 = 10$ MeV, and mono-pitch angle, $\theta_0 = 60^o$, RE beam. The scattered dots denote the numerical results taking into account full-orbit effects and spatial variation of the magnetic field for passing (shown in black) and trapped (shown in red) RE. The synchrotron radiation of trapped particles is quite different and stronger than the radiation due to passing particles. In particular, the spatial distribution of the radiation pattern exhibits strong “hot spots" at the tips of the banana orbits [3].

III. 3-D stochastic magnetic fields.

To study the role of magnetic islands and stochasticity on SR we computed full orbits of an ensemble of RE in a diverted DIII-D magnetic field computed using the MHD code NIMROD evolving the magnetic field (with a resistive-MHD Ohm law), a single fluid velocity, a

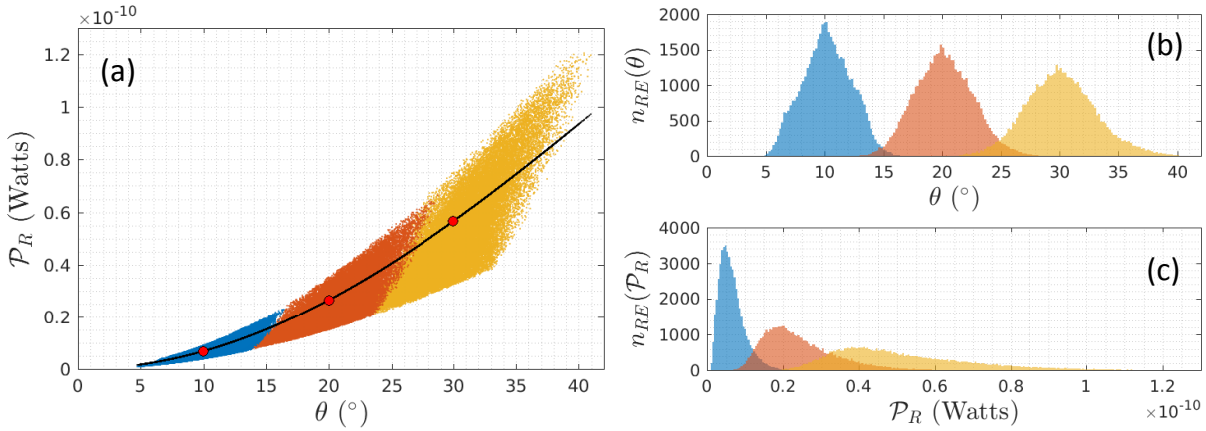

Figure 1: Synchrotron radiation power, $\mathscr{P}_R$, for passing particles in an axisymmetric magnetic field for mono-energetic ($\mathscr{E}_0 = 30$ MeV) runaway beams with initial pitch angles $\theta_0 = 10^o$ (blue), 20^o (orange) and 30^o (yellow) [3]. Panel (a) shows scatter plots in the (θ, $\mathscr{P}_R$) plane. The histograms in panels (b) and (c) show the number of runaways with a given pitch angle and the number of runaways with a given radiated power respectively at the end of the simulation.

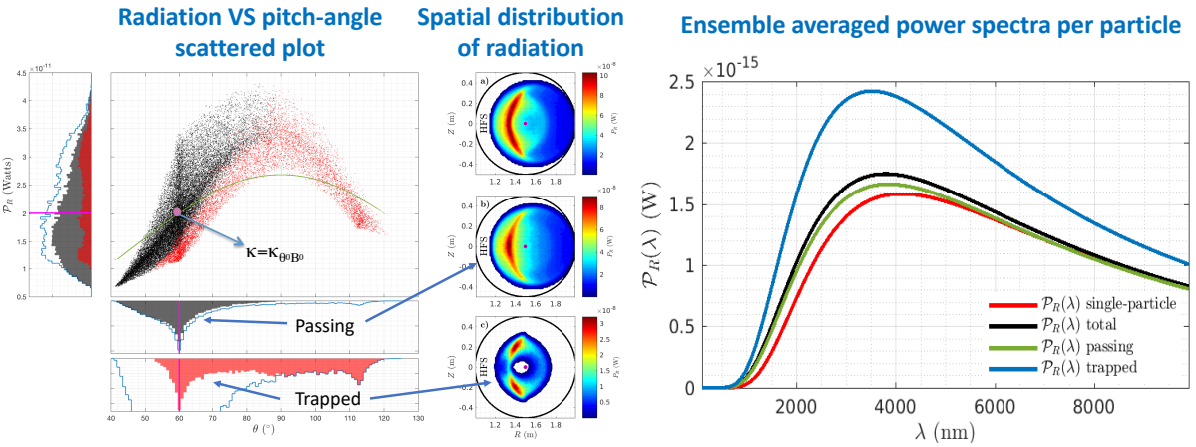

Figure 2: Trapped particle effects on synchrotron radiation in an axisymmetric magnetic field [3]. The main panel on the left shows scatter plots in the (θ, $\mathscr{P}_R$) plane. The histograms in the bottom and left sub-panels show the number of RE with a given θ and with a given $\mathscr{P}_R$ respectively at the end of the simulation. The plots on the middle column show the spatial radiation pattern in a poloidal plane for the total (top), passing only (middle), trapped only (bottom), RE populations. The corresponding synchrotron spectra are shown in the rightmost panel.

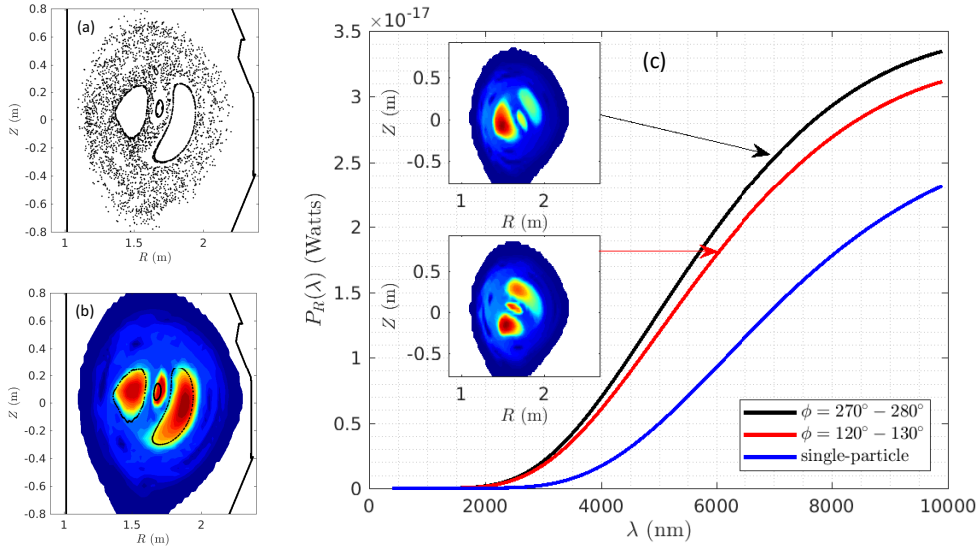

Figure 3: Synchrotron radiation of RE in 3-D magnetic fields with islands and stochasticity [3]. The top left panel shows the Poincare plot of the magnetic field and the bottom left panel the RE density. On the right panel, the blue line shows the spectrum neglecting orbit effects and assuming a constant magnetic field. The red and black lines show the spectra at the $\phi = 125^{\text{o}}$ and $\phi = 275^{\text{o}}$ poloidal planes respectively, taking into account full orbit effects as well as the three-dimensional structure of the magnetic field. The inserts show the spatial distribution of the instantaneous synchrotron radiation at the corresponding poloidal planes.

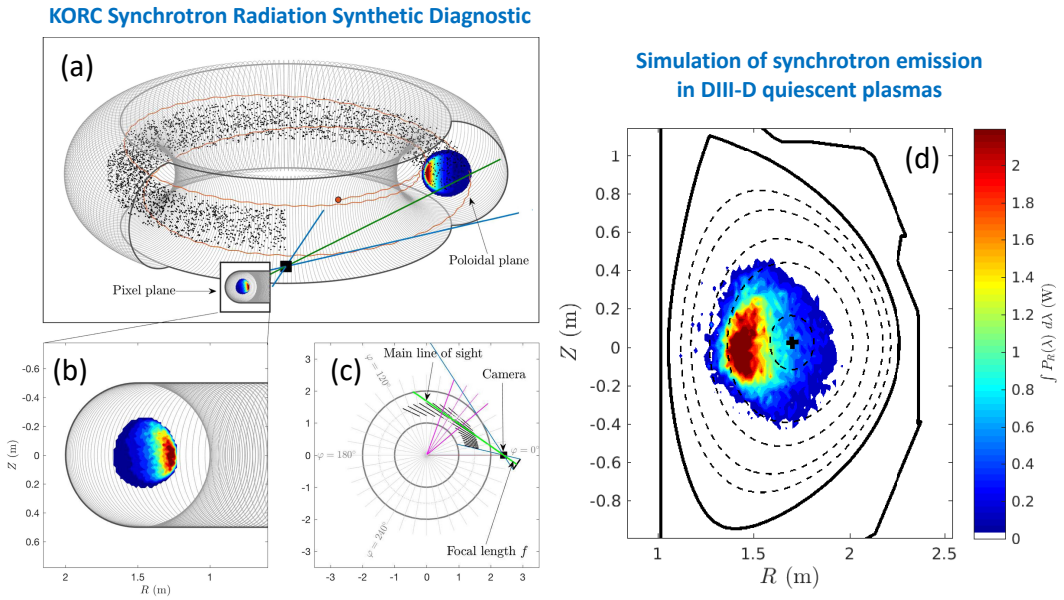

Figure 4: Left panel shows the synchrotron radiation synthetic diagnostic in KORC and right panel shows an application of the diagnostic for a DIII-D quiescent plasma [2,3].

single temperature, and a set of continuity equations for the deuterium ion density and the density of each charge state of an argon impurity used to model MPI (massive pellet injection) rapid plasma shutdown scenarios in DIII-D. In the calculations presented here we considered the magnetic field at the fixed time $t = 0.8$ ms when the radiative cooling triggers MHD instabilities with $n = 1$, 2 and 3 toroidal mode numbers resulting in widespread magnetic field stochasticity with some islands remaining at the core as shown in Fig. 3-(a). The initial condition consisted of a mono-energetic, $\mathscr{E}_0 = 13$ MeV, and mono-pitch, $\theta_0 = 8.6^{\text{o}}$, runaway beam uniformly distributed in a torus. The electrons in the stochastic region are lost and, as shown in Fig. 3-(b), the surviving electrons remain trapped in the magnetic islands. The impact of the 3-D structure of the magnetic field is shown in the instantaneous synchrotron radiation and power spectra shown in Fig. 3-(c) for two poloidal cross sections.

IV. KORC synchrotron radiation synthetic diagnostic

Panels (a), (b) and (c) in Fig. 4 show the SR synthetic diagnostic in KORC [2] and Fig. 4-(d) shows the application of the diagnostic to a quiescent plasmas in DIII-D [3]. RE experiments in these plasmas are well diagnose and controlled, and are thus valuable for validation studies. The KORC simulations presented here used a DIII-D EFIT reconstructed magnetic field and an energy distribution of runaways fitted to the experimental measurements. The computed spatial distribution of synchrotron radiation shows very good agreement with recent DIII-D quiescent plasmas experiments reported in Ref. [4].

Acknowledgments.

We thank Carlos Paz-Soldan for valuable discussions on synchrotron emission of runaway electrons in DIII-D quiescent plasmas. This work was sponsored by the Oak Ridge National Laboratory, managed by UT-Battelle, LLC, for the U.S. Department of Energy under contract DE-AC05-00OR22725.

References

[1] L. Carbajal, D. del-Castillo-Negrete, D. Spong, S. Seal, and L. Baylor, Phys. of Plasmas **24**, 042512 (2017).

[2] L. Carbajal and D. del-Castillo-Negrete, Plasma Phys. and Control. Fusion **59**, 124001 (2017).

[3] D. del-Castillo-Negrete, L. Carbajal, D. Spong and V. Izzo, Phys. Plasmas **25**, 056104 (2018).

[4] Paz-Soldan, et al., Phys. Plasmas **25**, 056105 (2018).